*electronics*

*Article*

# A Compact mmWave MIMO Antenna for Future Wireless Networks

**Muhammad Imran Khan [1,*], Sarmadullah Khan [2], Saad Hassan Kiani [3,4], Naser Ojaroudi Parchin [5,*], Khalid Mahmood [6], Umair Rafique [7] and Muhammad Mansoor Qadir [8]**

1 Department of Electrical Engineering, CECOS University, Peshawar 25000, Pakistan
2 School of Computer Science and Informatics, De Montfort University, The Gateway, Leicester LE1 9BH, UK
3 Department of Electrical Engineering, IIC University of Technology, Phnom Penh 121206, Cambodia
4 Smart Systems Engineering Laboratory, College of Engineering, Prince Sultan University, Riyadh 11586, Saudi Arabia
5 School of Engineering and the Built Environment, Edinburgh Napier University, Edinburgh EH10 5DT, UK
6 Department of Electrical Engineering, Abasyn University, Peshawar 25000, Pakistan
7 Department of Information Engineering, Electronics and Telecommunications, Sapienza University of Rome, 00184 Rome, Italy
8 Department of Computer Science, Iqra National University, Peshawar 25000, Pakistan
* Correspondence: imran@cecos.edu.pk (M.I.K.); n.ojaroudiparchin@napier.ac.uk (N.O.P.)

**Abstract:** This article presents a four-element multiple-input multiple-output (MIMO) antenna design for next-generation millimeter-wave (mmWave) communication systems. The single antenna element of the MIMO systems consists of a T-shaped and plow-shaped patch radiator designed on an ultra-thin Rogers RT/Duroid 5880 substrate. The dimensions of the single antenna are 10 × 12 mm$^2$. The MIMO system is designed by placing four elements in a polarization diversity configuration whose overall dimensions are 24 × 24 mm$^2$. From the measured results, it is observed that the MIMO antenna provides 9.23 GHz impedance bandwidth ranging from 22.43 to 31.66 GHz. In addition, without the utilization of any decoupling network, a minimum isolation of 25 dB is achieved between adjacent MIMO elements. Furthermore, the proposed MIMO antenna system is fabricated, and it is noted that the simulated results are in good agreement with the measured results. Through the achieved results, it can be said that the proposed MIMO antenna system can be used in 5G mmWave radio frequency (RF) front-ends.

**Keywords:** MIMO; mmWave; plow-shape; polarization diversity



**Citation:** Khan, M.I.; Khan, S.; Kiani, S.H.; Ojaroudi Parchin, N.; Mahmood, K.; Rafique, U.; Qadir, M.M. A Compact mmWave MIMO Antenna for Future Wireless Networks. *Electronics* **2022**, *11*, 2450. https://doi.org/10.3390/electronics11152450

Academic Editor: Christos J. Bouras

Received: 27 June 2022
Accepted: 3 August 2022
Published: 6 August 2022



## 1. Introduction

The new communication era is based on fifth-generation (5G) technology, which has been deemed the fastest data-rate-providing technology when compared to third-generation (3G) and fourth-generation (4G) technologies. The International Telecommunication Union (ITU) divided the 5G communication spectrum into two parts. One of them is named the sub-6 GHz spectrum [1], whereas the second one is called the millimeter-wave (mmWave) spectrum [2–4]. The reason for choosing sub-6 GHz spectrum is to achieve high data rates with existing communication technologies [5], but the antenna size is quite large and also the gain of the antenna will be low [6]. In contrast to this, at mmWave frequency bands, the small wavelength provides an extra advantage for designing compact antennas for 5G communication systems. In addition, the higher frequency bands provide large bandwidth, which ultimately leads to achieving a high data rate [7,8]. At mmWave spectrum, the propagation loss is high due to small wavelengths [9,10], and this problem can be solved by designing high-gain antennas. In addition, high data rates can be achieved by utilizing multiple-input multiple-output (MIMO) technology. For this purpose, many researchers have reported different MIMO antenna designs in the literature for the mmWave spectrum.

In [11], a coplanar waveguide (CPW)-fed antenna array was presented for mmWave networks. The authors designed a linear MIMO array by utilizing a T-shaped radiator with a defected ground plane. The use of a defected ground plane enhanced the isolation between antenna elements, which tends to achieve high channel capacity, but it reduces the directivity of the MIMO antenna. In [12], a four-element MIMO antenna was designed for mmWave applications. A nature-inspired patch radiator and a partial ground plane with a semi-circular shell was used to achieve a wideband response. The presented results show that the single antenna provides a bandwidth of 4 GHz in the frequency range of 26–30 GHz. In the MIMO configuration, a minimum isolation of 24 dB was observed between the MIMO elements. In [13], a quad-port MIMO antenna design was presented for 5G mmWave applications. The MIMO's single element consists of a $1 \times 2$ array of patch radiators. To achieve wideband response and high isolation, a defected ground structure (DGS) configuration was utilized. It was observed that the use of DGS tends to achieve a wideband response from 25.5 to 29.6 GHz, whereas the isolation between antenna elements was noted to be less than 10 dB. The same kind of MIMO configuration was designed in [14]. In this design, the authors used a slotted zig-zag decoupling structure to achieve >25 dB of isolation in the band of interest. In [15], a tree-shaped patch-based MIMO antenna system was reported for future mmWave communication systems. The radiating structure was designed in such a way so that it can provide a wideband impedance bandwidth ranging from 23 to 40 GHz. It was also observed that the designed patch antenna offered a high gain of 11.45 dBi in the band of interest.

In [16], a MIMO antenna was designed by using the design technique presented in [13]. The presented MIMO antenna resonates well in the frequency range of 24.55–26.5 GHz. To achieve high isolation (>25 dB), an array of metasurface was placed above the MIMO antenna. The same kind of technique was utilized in [17]. In this design, the authors used a novel patch shape with a partial ground plane to achieve a wideband response ranging from 23.5 to 29.4 GHz. Furthermore, the isolation between the antenna elements was noted to be >20 dBi for the entire operating bandwidth. For high gain, a $2 \times 2$ array of metasurface was used and achieved a peak gain of 10.44 dBi. Although the MIMO structures provide high isolation and high gain, their bulky configuration restricts their use in compact communication devices. In [18], a novel MIMO antenna configuration was adopted to achieve high isolation. The MIMO design was able to operate at a very wideband frequency range of 36.83–40.0 GHz. Furthermore, an isolation of >18 dB was achieved with a peak gain of 6.5 dBi. However, the presented configuration can only be used in arbitrary-shaped communication devices. In [19], three-element and four-element MIMO antenna designs were presented for 5G mmWave applications. The authors used an inverted-L shaped patch element to achieve a wideband response in the frequency range of 26–40 GHz. In the three-element MIMO design, they employed slots in the ground plane to achieve an isolation of >15 dB between antenna elements, whereas in the four-element design, semi-arc was designed within the slots to obtain an isolation of >22 dB. Although the presented designs offer wideband response and high isolation, they suffer due to low antenna efficiency.

Based on the above-presented discussion, in this article, a T-shaped and plow-shaped patch-based wideband four-element MIMO antenna design is presented for mmWave communication systems. The proposed design is based on a polarization diversity technique and occupies an overall size of $24 \times 24$ mm$^2$, which enables its use in compact communication devices. The wideband response is achieved by utilizing a partial ground plane with a square notch. It is observed from the presented results that the MIMO antenna operates well from 22.43 to 31.66 GHz and provides measured impedance bandwidth of 9.23 GHz. Furthermore, without the use of any decoupling or isolation enhancement network, an isolation of 25 dB is achieved between adjacent antenna elements.

## 2. Antenna Design

### *2.1. Single Element*

The proposed single antenna element design is shown in Figure 1. The front-side of the antenna consists of a T-shaped and plow-shaped patch radiator (see Figure 1a), whereas the back side consists of a partial ground plane with a square notch, as shown in Figure 1b. The plow-shape is comprised of a T-shaped resonator and two extended strips bent at 15°. The partial ground plane is utilized to achieve wideband repose in the band of interest, whereas the square notch is used to enhance the impedance matching. A low-loss ultra-thin Rogers RT/Duroid 5880 dielectric substrate is used for the design of an antenna. The thickness of the dielectric substrate is chosen to be 0.254 mm, and its relative permittivity is equal to 2.2. The overall dimensions of the proposed plow-shaped antenna are noted to be 10 × 12 $mm^2$. For the feeding of a plow-shaped patch, a 50 Ω microstrip feeding line is used, whose length and width are equal to 6.75 mm and 0.787 mm, respectively (see Figure 1a). The feed line length is extended to use the connector in an efficient manner. The rest of the design parameters with their respective values are shown in Figure 1.

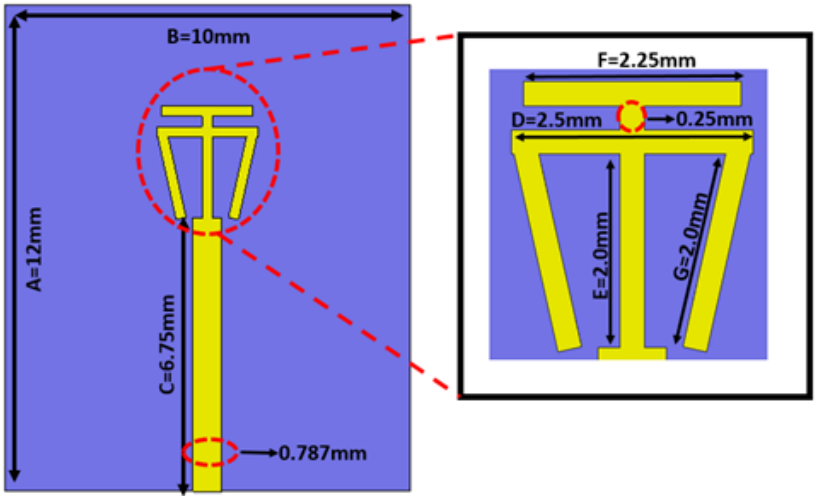


(**a**)

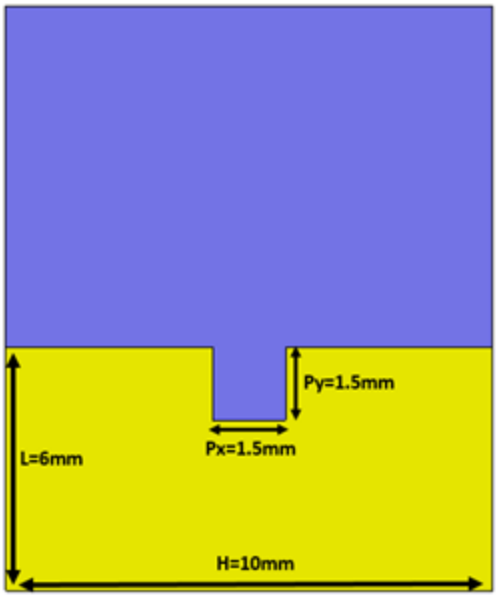


(**b**)

**Figure 1.** Proposed single antenna element (**a**) front-view and (**b**) back-view.

The simulated reflection coefficient ($S_{11}$) response of the proposed single antenna element is illustrated in Figure 2a. One can note from the figure that, according to −10 dB impedance bandwidth criteria, the antenna operates well from 22.24 to 31.76 GHz, providing an impedance bandwidth of 9.52 GHz and a fractional bandwidth of 35.25%. The simulated radiation and total efficiency responses of the proposed antenna are shown in Figure 2b. The radiation efficiency is noted to be >95% for the desired operating bandwidth. On the other hand, the total efficiency fluctuates in the range of 83–97%. In addition, the proposed antenna realized gain is shown in Figure 2c. It is noted that the gain of the antenna varies from 2 to 3.5 dBi in the operating bandwidth (see Figure 2c).

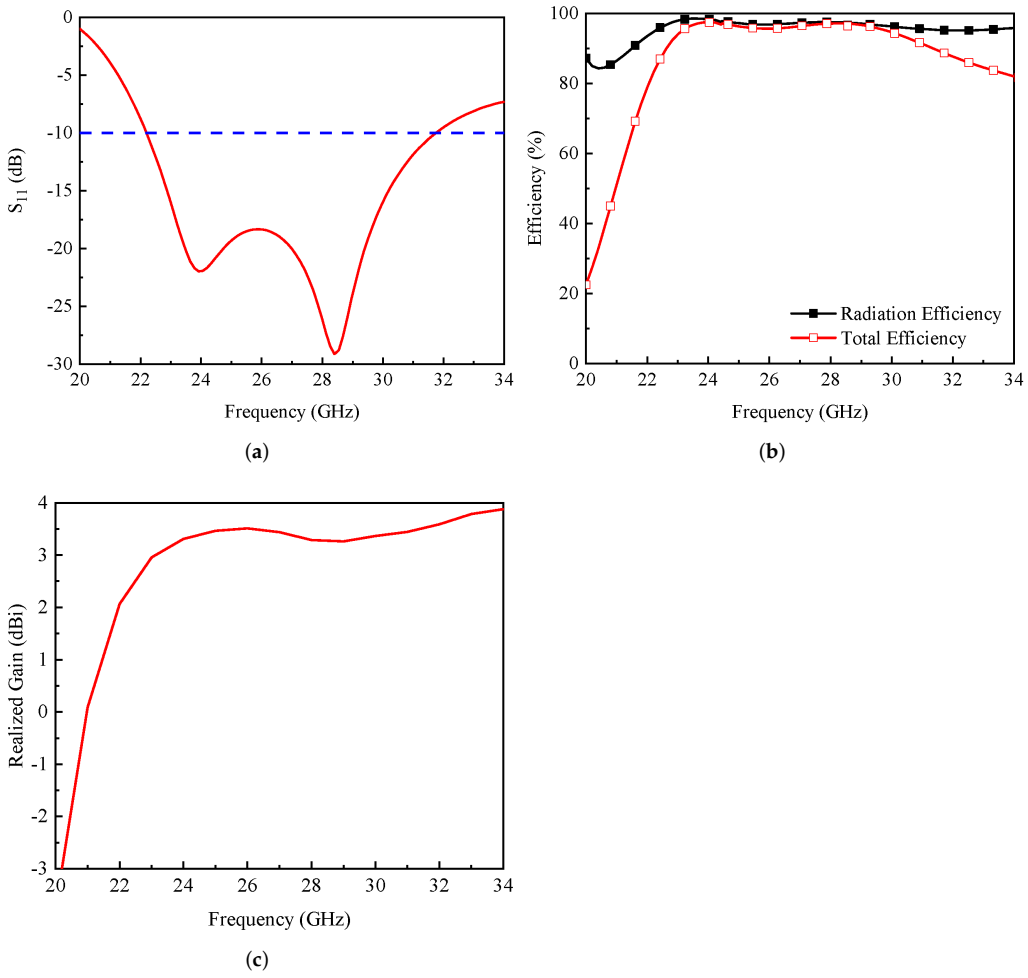


**Figure 2.** Simulated (**a**) $S_{11}$, (**b**) radiation and total efficiency, and (**c**) realized gain of the proposed antenna.

The single antenna element was developed through a series of parametric studies. The parameters optimized to obtain the desired response are: square notch modeling in the ground plane, the angle of the open strips attached at both ends of the plow-shaped resonator, the horizontal strip of the plow-shaped resonator, and the length of the T-shaped resonator. Figure 3a shows the effect of ground slot on an antenna's performance. The parameter "Px" value has been changed from 1.3 to 1.7 mm. As the value of "Px" increases, a shift in the lower frequency is observed, as shown in Figure 3a. The optimum response is achieved at Px = 1.5 mm, where the antenna provides acceptable bandwidth and impedance matching (see Figure 3a). For values greater than 1.5 mm, the bandwidth of the antenna is going to decrease, as depicted in Figure 3a.

Figure 3b shows the parametric modeling of the side suspended strips whose length is named as "G". The performance is assessed by changing the rotation angle of the

strips from 0° to 20°. As seen from Figure 3b, this angle plays a vital role in producing a desired response. As the angle increases, an increase in impedance bandwidth is observed (see Figure 3b). From the presented study, the desired response is achieved at an angle of 15° angle, as shown in Figure 3b. The effect of parameter "D" on antenna's performance is depicted in Figure 3c. As the value of "D" changed from 2.3 to 2.7 mm, an improved impedance matching is observed on the expense of reduce antenna bandwidth. For D = 2.3 mm, the antenna offers wide impedance bandwidth but provides low impedance matching in the band of interest (see Figure 3c). The optimized response is achieved for D = 2.5 mm, as shown in Figure 3c.

Figure 3d depicts the effect of T-shaped resonator length "F" on the antenna's performance. As the length of the T-shaped resonator increases, a drastic change is observed in the impedance bandwidth, as shown in Figure 3d. For F = 1.75 mm, the antenna provides a wide impedance bandwidth, but the impedance matching is low. An acceptable performance in terms of bandwidth and impedance matching is achieved for F = 2.25 mm (see Figure 3d).

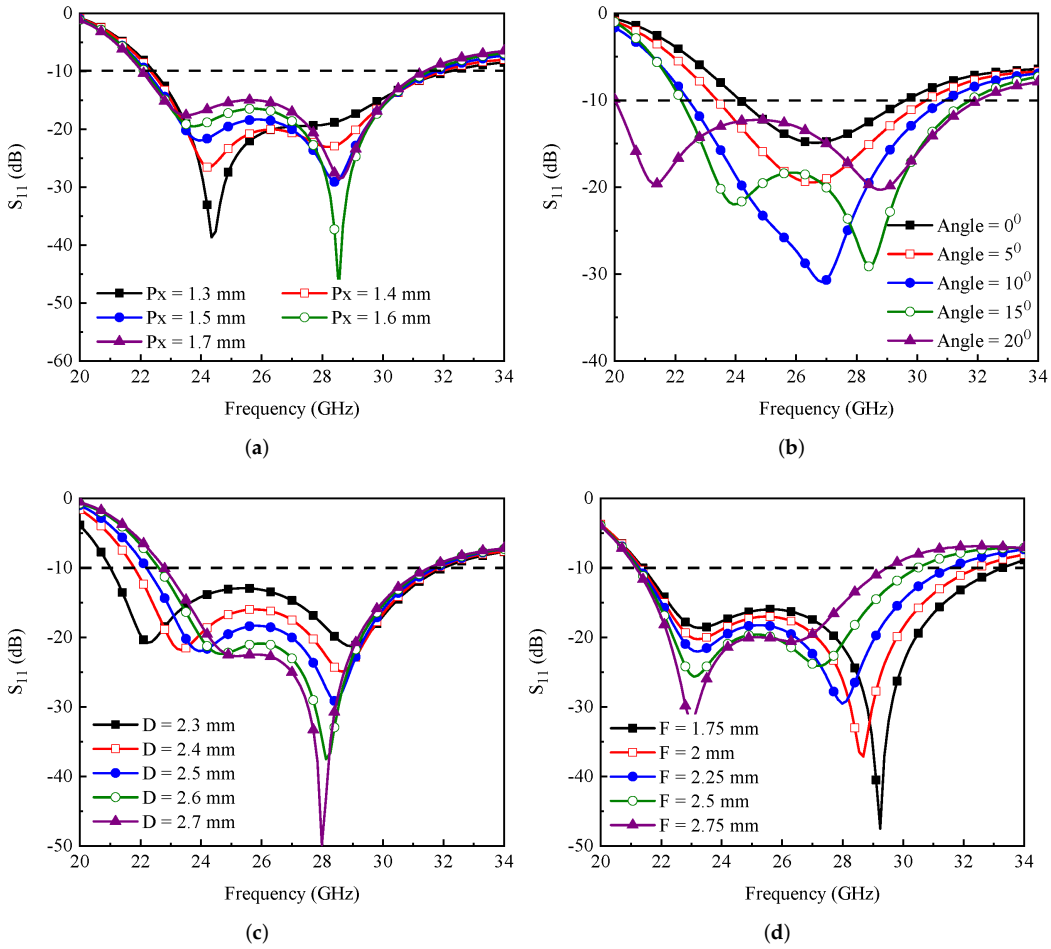


**Figure 3.** Effect of (**a**) square notch width "Px", (**b**) strip angle, (**c**) plow-shaped horizontal strip "D", and (**d**) T-shaped resonator length "F" on antenna's performance.

### *2.2. MIMO Antenna Configuration*

The proposed single antenna element was transformed into a four-element MIMO configuration to achieve a high data rate and high channel capacity in the mmWave spectrum. Figure 4 shows the design of the proposed MIMO antenna. The MIMO antenna is designed by placing the above-presented antenna element in a polarization diversity configuration, as shown in Figure 4a, whereas the back side consists of independent partial

ground planes loaded with a square notch (see Figure 4b). The dimensions of the proposed MIMO antenna are noted to be 24 × 24 mm$^2$. From the figure, one can observe that there is no decoupling network designed between the antenna elements to achieve high isolation.

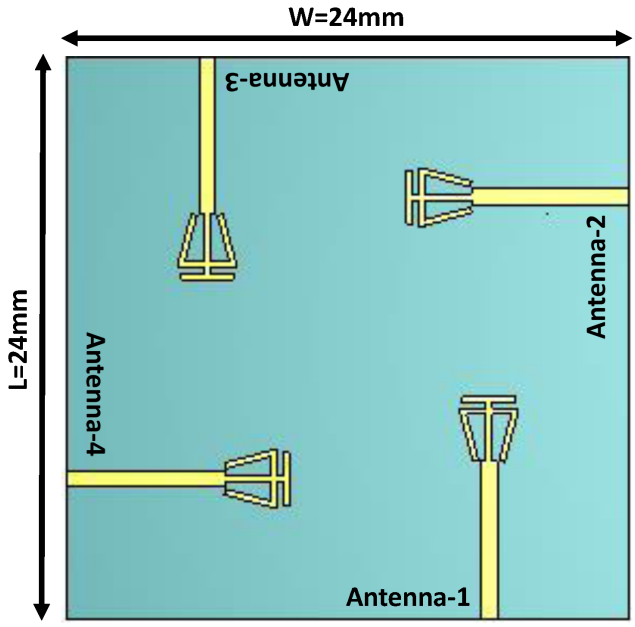


(**a**)

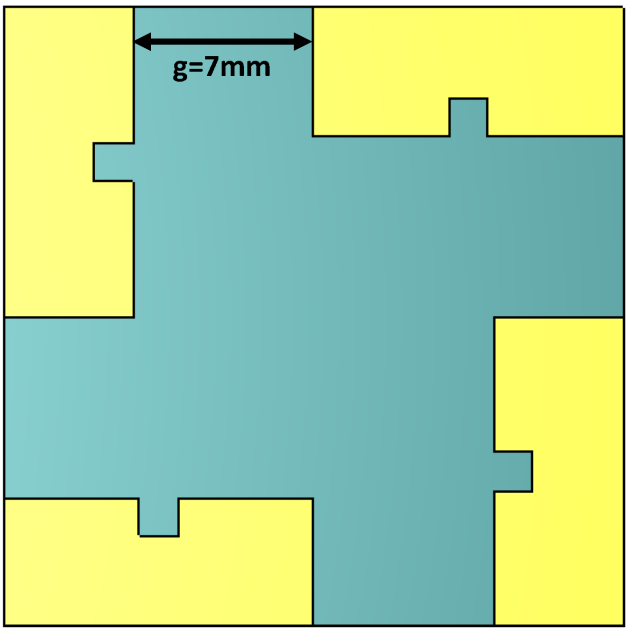


(**b**)

**Figure 4.** Proposed MIMO antenna (**a**) front-view and (**b**) back-view.

## 3. Experimental Results and Discussion

### *3.1. S-Parameters*

To verify the simulated data, the proposed MIMO antenna was fabricated and tested using an in-house facility. Figure 5 shows the proposed antenna fabricated prototype. The S-parameters of the proposed MIMO antenna, both simulated and measured, are shown in Figure 6. For simplicity, the reflection coefficients of only two antenna elements are shown. Figure 6a shows the simulated and measured reflection coefficients of antenna-1 and

antenna-2. From the simulated reflection coefficients, shown in Figure 6a, it is observed that antenna-1 resonates from 22.2 to 31.66 GHz, whereas antenna-2 operates in the frequency range of 22.4–32.57 GHz. On the other hand, the measured results show that antenna-1 and antenna-2 provide impedance bandwidths ranging from 22.95 to 31.53 GHz and 22.43 to 31.66 GHz, respectively (see Figure 6a). The simulated and measurement isolation results are depicted in Figure 6b. The isolation between adjacent antenna elements is noted to be greater than 25 dB for the entire operating bandwidth. The discrepancies between the results may arise due to SMA connector losses, fabrication tolerances, and indoor scattering environments.

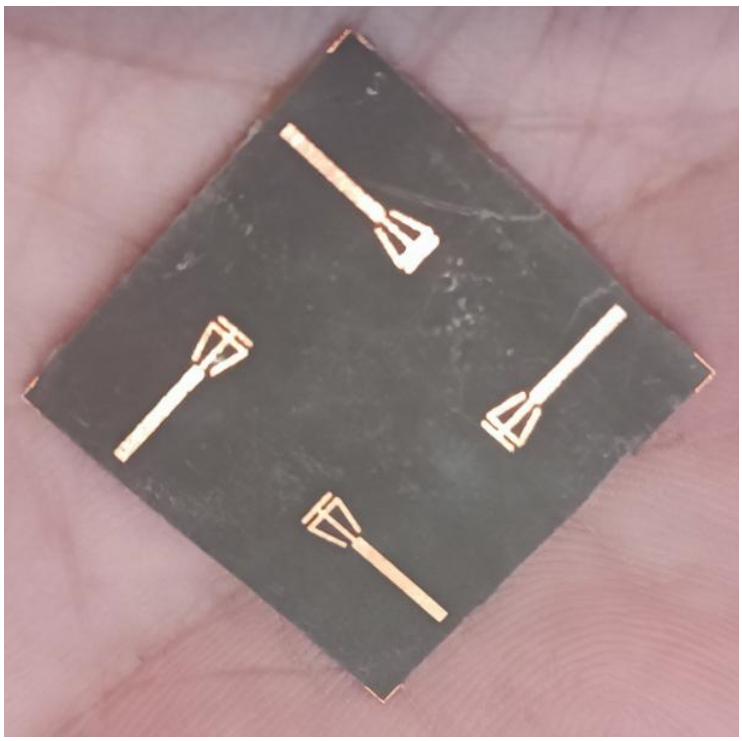

**Figure 5.** Fabricated prototype of proposed MIMO antenna.

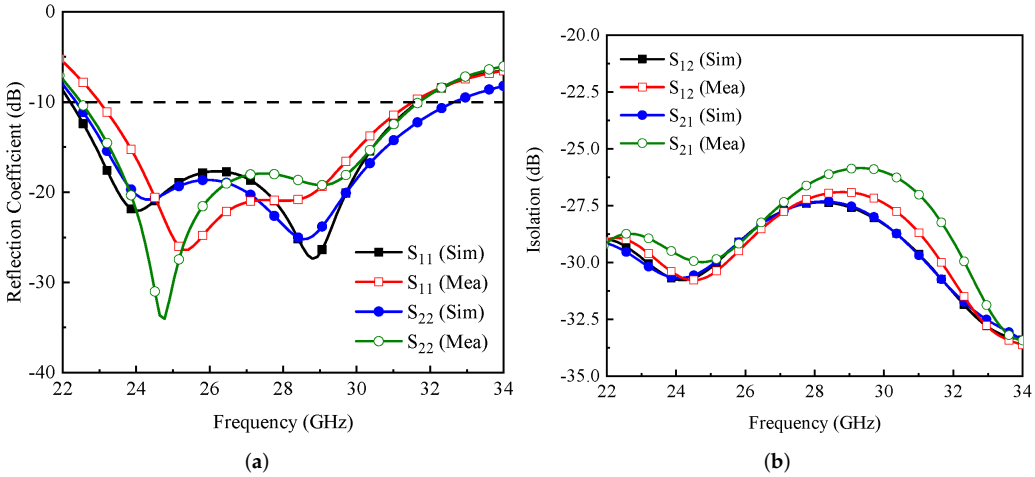


**Figure 6.** Simulated and measured (**a**) reflection coefficients and (**b**) port isolations of the proposed MIMO antenna.

### *3.2. Radiation Characteristics*

The far-field radiation characteristics of the presented MIMO antenna are assessed using a traditional method. As a reference antenna, a dual-ridge horn antenna with a

frequency range of 15–40 GHz is employed, and the designed MIMO antenna is mounted on a turntable that is positioned on the opposite side. RF absorbers are used to cover the anechoic chamber's walls in order to eliminate reflections.

The simulated and measured gain patterns for $\phi = 0^\circ$ and $\phi = 90^\circ$ are shown in Figure 7. The radiation patterns are extracted at 24.5 GHz. It is observed from Figures 7a,c that antenna-1 and antenna-3 offer omnidirectional radiation properties for $\phi = 0^\circ$ and bi-directional (monopole-like) radiation characteristics for $\phi = 90^\circ$. The same kinds of radiation patterns are observed for antenna-2 and antenna-4 (see Figures 7b,d). In this case, the proposed MIMO antenna shows polarization diversity behavior, as shown in Figures 7b,d. In addition to this, the proposed MIMO antenna system is also able to provide pattern diversity in both the planes at the same time, which is clear from the results of Figure 7. This effect can also be observed from Figure 8 where three-dimensional (3-D) radiation characteristics of the proposed antenna are plotted. From the results of Figure 8, it can also be observed that the gain of the MIMO antenna varies in the range of 5.23–5.46 dBi.

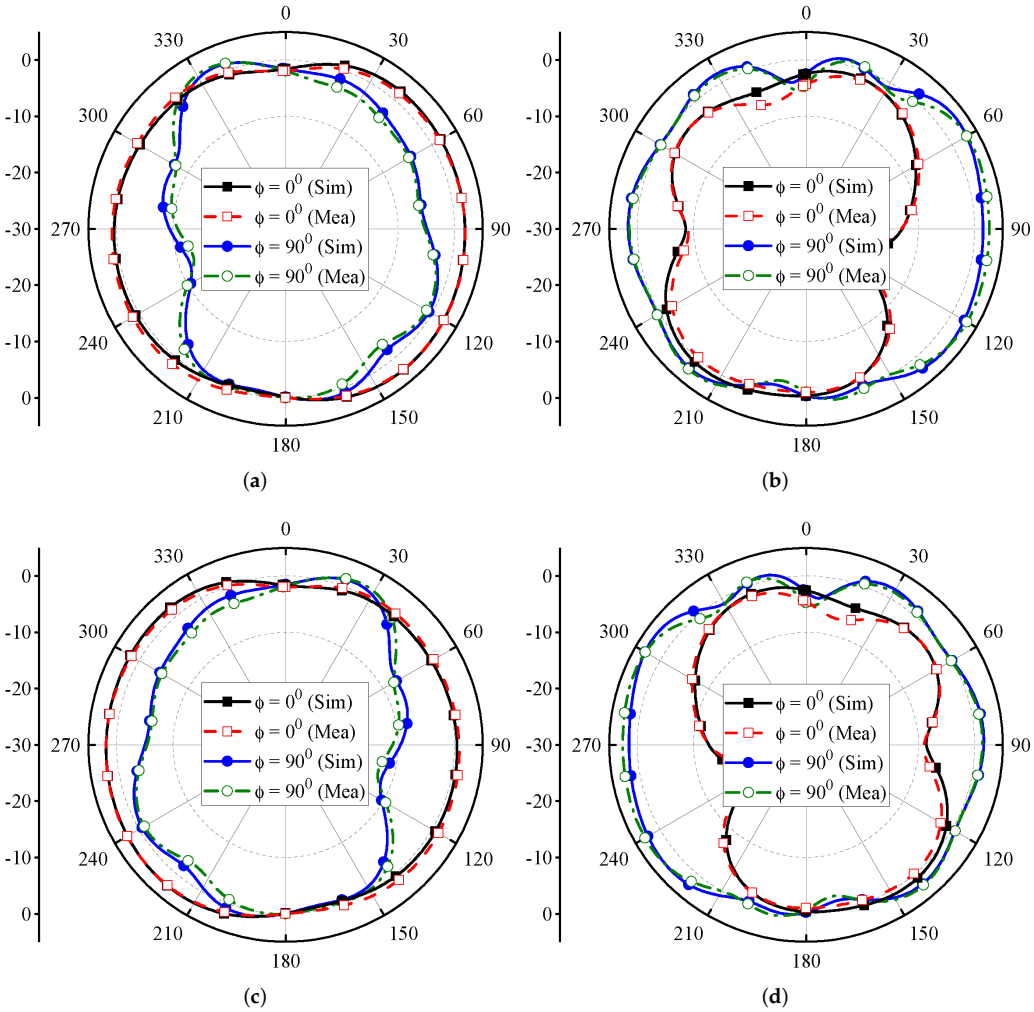


**Figure 7.** Far-field radiation characteristics of the proposed MIMO antenna at 24.5 GHz for (**a**) antenna-1, (**b**) antenna-2, (**c**) antenna-3, and (**d**) antenna-4.

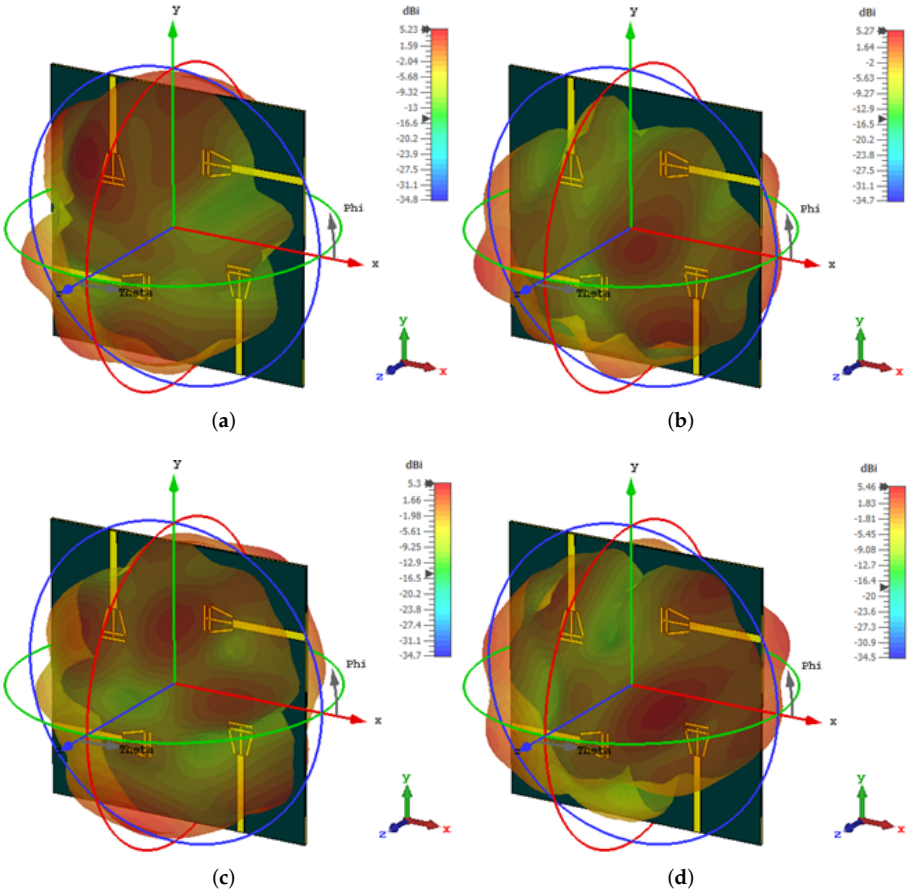


**Figure 8.** 3-D radiation patterns of the proposed MIMO antenna at 24.5 GHz for (**a**) antenna-1, (**b**) antenna-2, (**c**) antenna-3, and (**d**) antenna-4.

### *3.3. Total Efficiency and Realized Gain*

In Figure 9a, the total efficiency of all the antenna elements is plotted, whereas the overall MIMO realized gain is depicted in Figure 9b. From Figure 9a, it can be observed that the total efficiency of the antenna elements is greater than 85% for the entire operating bandwidth. On the other hand, the simulated gain of the MIMO antenna fluctuates in the range of 5.23–5.46 dBi, whereas the measured gain varies from 4.98 to 5.66 dBi (see Figure 9b).

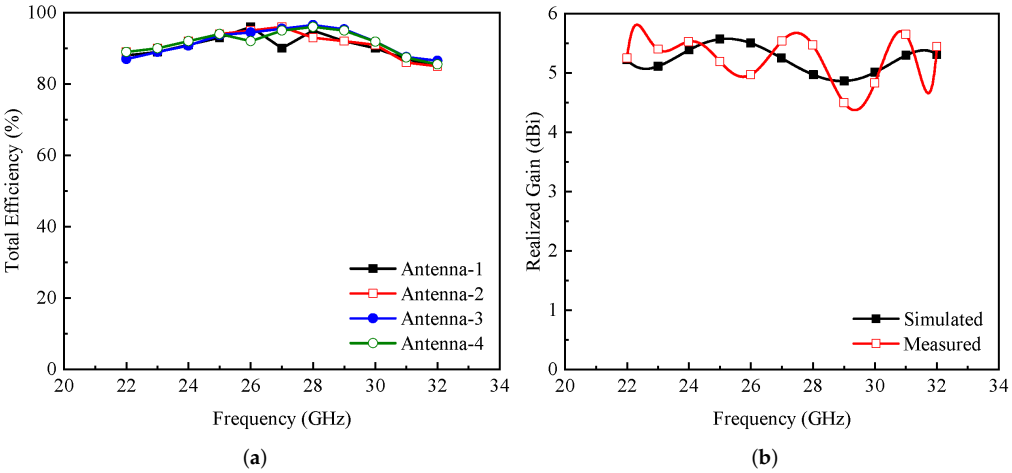


**Figure 9.** (**a**) Total efficiency and (**b**) realized gain of the proposed MIMO antenna.

### *3.4. Surface Current*

The simulated surface current distribution of the proposed MIMO antenna for all the antenna elements is depicted in Figure 10. It can be noted that for all antenna elements, maximum current is distributed around the feedline, the radiating structure, and the square notch etched on the ground plane. So, it can be said that the square notch plays an important role in achieving a wideband response.

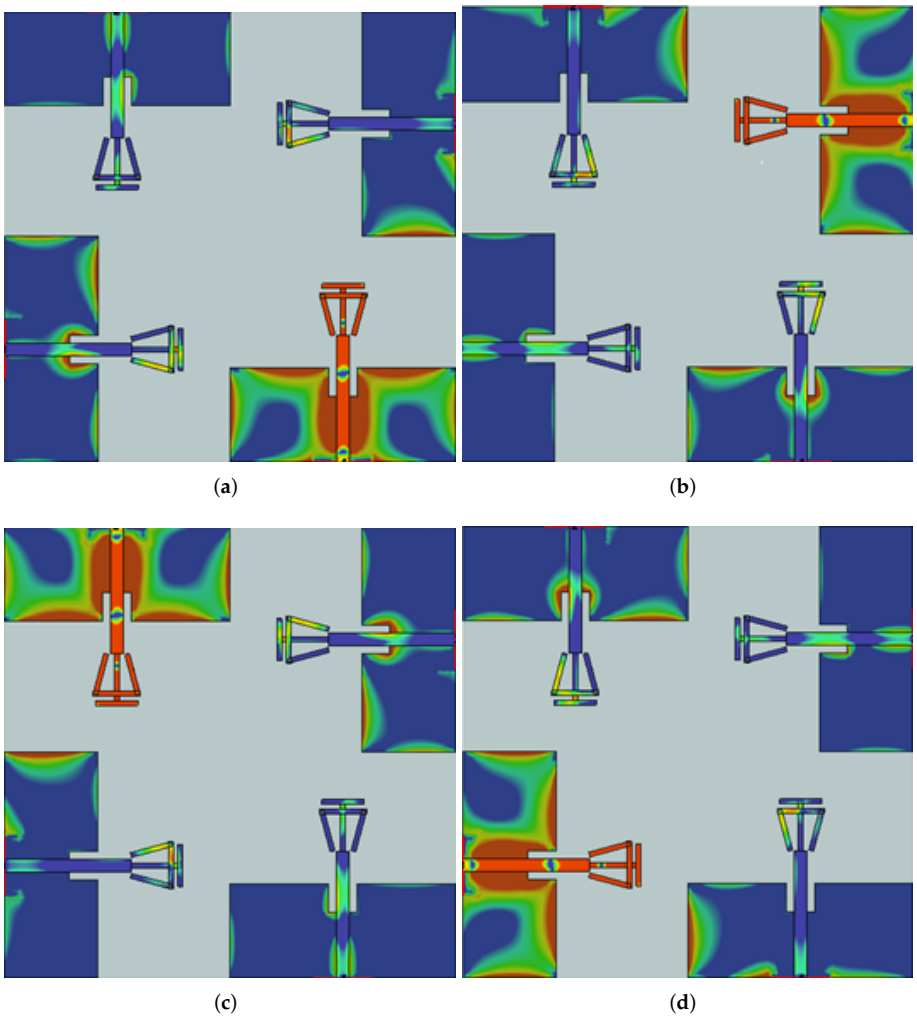


**Figure 10.** Surface current distribution for (**a**) antenna-1, (**b**) antenna-2, (**c**) antenna-3, and (**d**) antenna-4.

## 4. MIMO Parameters

MIMO diversity parameters are important to discuss while designing a MIMO antenna system. These MIMO parameters include envelope correlation coefficient (ECC), diversity gain (DG), and mean effective gain (MEG). ECC is the measure of how well the antennas are isolated and can be calculated using the far-field radiation characteristics of the MIMO antenna [1]. In Figure 11a, the ECC of the presented MIMO antenna system is presented. Within the desired operating band, the ECC value is observed to be less than 0.008, which follows the standard value of $\leq$0.5. The low value of ECC also ensures that the proposed MIMO system will have independent channel operation. Furthermore, the DG of the designed MIMO antenna is shown in Figure 11b. The DG can be calculated through ECC as mentioned in [1]. For the presented MIMO antenna system, the DG value is greater than 9.95 dB for the band of interest (see Figure 11b).

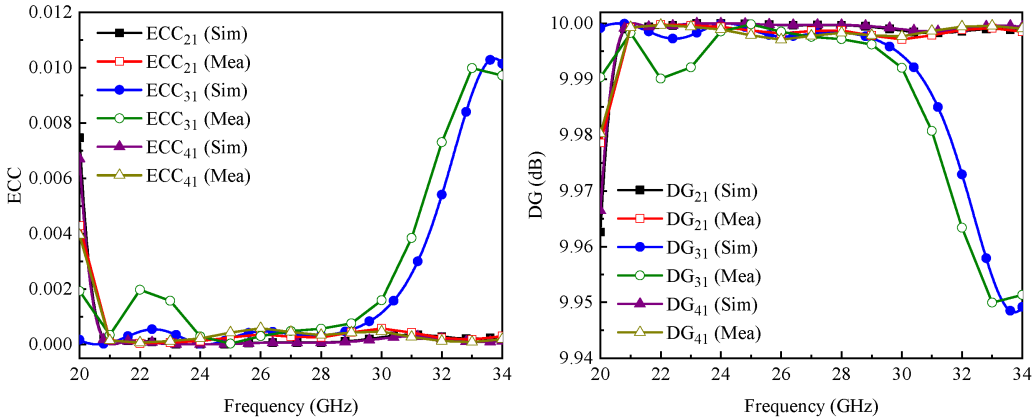


**Figure 11.** (**a**) Envelope correlation coefficient and (**b**) diversity gain of the proposed MIMO antenna.

MEG is another important MIMO parameter, which is calculated using the equation given in [3] at frequencies of 28 GHz, 28.5 GHz, and 29 GHz, respectively, for all the four antenna elements. MEG actually provides information about how much power is received by each antenna in the MIMO system. Through Table 1, the MEG of the proposed MIMO antenna system is less than −3 dB, which satisfies the convention.

**Table 1.** Mean effective gain of the proposed MIMO antenna.

| Frequency (GHz) | MEG1 | MEG2 | MEG3 | MEG4 |
|---|---|---|---|---|
| 28 | −3.50 | −3.21 | −3.26 | −3.10 |
| 28.5 | −3.48 | −3.17 | −3.25 | −3.33 |
| 29 | −2.87 | −3.1 | 3.47 | −3.88 |

The comparison among previously presented and designed MIMO antenna systems is listed in Table 2. It is noted from the table that the size of the proposed MIMO antenna is small compared to the designs of [13,14,16,19]. Furthermore, the proposed MIMO antenna system offers high bandwidth and acceptable isolation performance compared to the designs reported in [12–14,16,17].

**Table 2.** Comparison among previously presented and proposed mmWave MIMO antennas.

| Ref. | Size ($mm^2$) | Bandwidth (GHz) | Isolation (dB) | Efficiency (%) | Gain (dBi) | ECC |
|---|---|---|---|---|---|---|
| [12] | 25 × 15 | 3 | 25 | >90 | 8 | <0.001 |
| [13] | 35 × 30 | 4 | >20 | >80 | 8.3 | <0.04 |
| [14] | 35 × 30 | 1 | >30 | >80 | 12 | <0.0008 |
| [16] | 43 × 30 | 1.95 | >30 | – | 10.21 | <0.0008 |
| [17] | 24 × 24 | 5.9 | >25 | >80 | 10.44 | <0.01 |
| [19] | 30 × 30 | 14 | >20 | 60 | 8 | <0.018 |
| This Work | 24 × 24 | 9.23 | >25 | >85 | 5.66 | <0.008 |

## 5. Conclusions

In this article, a wideband four-element MIMO antenna system is presented for mmWave communication systems. The MIMO antenna system is designed in such a way that it can provide both pattern and polarization diversity at the same time. From the results, it is noted that the bandwidth of the proposed MIMO antenna system is noted to be 9.23 GHz, ranging from 22.43 to 31.66 GHz. The isolation between adjacent elements and diagonal elements is observed to be >25 dB and >18.5 dB, respectively. The MIMO parameters are also evaluated and their values lie within an acceptable range. Therefore, the proposed MIMO antenna system could be used as a potential candidate for future mmWave wireless systems.

**Author Contributions:** Conceptualization, S.H.K. and N.O.P.; methodology, M.I.K. and K.M.; software, S.H.K. and K.M.; validation, N.O.P. and K.M.; formal analysis, N.O.P. and U.R.; investigation, S.K.; resources, S.K. and N.O.P.; writing—original draft preparation, S.H.K. and M.M.Q.; writing—review and editing, N.O.P., U.R., and M.M.Q.; visualization, U.R. and M.M.Q.; supervision, S.H.K. and N.O.P.; project administration, K.M. and U.R.; funding acquisition, N.O.P. and U.R. All authors have read and agreed to the published version of the manuscript.

**Funding:** This project received no external funding.

**Conflicts of Interest:** The authors declare no conflict of interest.

## References

1. Rafique, U.; Khan, S.; Ahmed, M.M.; Kiani, S.H.; Abbas, S.M.; Saeed, S.I.; Alibakhshikenari, M.; Dalarsson, M. Uni-Planar MIMO Antenna for Sub-6 GHz 5G Mobile Phone Applications. *Appl. Sci.* **2022**, *12*, 3746. [CrossRef]
2. Munir, M.E.; Al Harbi, A.G.; Kiani, S.H.; Marey, M.; Parchin, N.O.; Khan, J.; Mostafa, H.; Iqbal, J.; Khan, M.A.; See, C.H.; et al. A New mm-Wave Antenna Array with Wideband Characteristics for Next Generation Communication Systems. *Electronics* **2022**, *11*, 1560. [CrossRef]
3. Kiani, S.H.; Alharbi, A.G.; Khan, S.; Marey, M.; Mostafa, H.; Khan, M.A. Wideband Three Loop Element Antenna Array for Future 5G mmwave Devices. *IEEE Access* **2022**, *10*, 22472–22479. [CrossRef]
4. Luo, Y.; Shen, Y.; Cai, X.; Qian, F.; Xu, S.; Cui, H.; Yang, G. Substrate integrated coaxial line design for mmWave antenna with multilayer configuration. *Int. J. RF Microw. Comput.-Aided Eng.* **2022**, *32*, e23090. [CrossRef]
5. Kiani, S.H.; Iqbal, A.; Wong, S.W.; Savci, H.S.; Alibakhshikenari, M.; Dalarsson, M. Multiple Elements MIMO Antenna System With Broadband Operation for 5th Generation Smart Phones. *IEEE Access* **2022**, *10*, 38446–38457. [CrossRef]
6. Farasat, M.; Thalakotuna, D.N.; Hu, Z.; Yang, Y. A review on 5G sub-6 GHz base station antenna design challenges. *Electronics* **2021**, *10*, 2000. [CrossRef]
7. Ishteyaq, I.; Muzaffar, K. Multiple input multiple output (MIMO) and fifth generation (5G): An indispensable technology for sub-6 GHz and millimeter wave future generation mobile terminal applications. *Int. J. Microw. Wirel. Technol.* **2021**, *14* 932–948. [CrossRef]
8. Wang, Y.; Li, J.; Huang, L.; Jing, Y.; Georgakopoulos, A.; Demestichas, P. 5G mobile: Spectrum broadening to higher-frequency bands to support high data rates. *IEEE Veh. Technol. Mag.* **2014**, *9*, 39–46. [CrossRef]
9. Osseiran, A.; Boccardi, F.; Braun, V.; Kusume, K.; Marsch, P.; Maternia, M.; Queseth, O.; Schellmann, M.; Schotten, H.; Taoka, H.; et al. Scenarios for 5G mobile and wireless communications: The vision of the METIS project. *IEEE Commun. Mag.* **2014**, *52*, 26–35. [CrossRef]
10. Sulyman, A.I.; Nassar, A.T.; Samimi, M.K.; MacCartney, G.R.; Rappaport, T.S.; Alsanie, A. Radio propagation path loss models for 5G cellular networks in the 28 GHz and 38 GHz millimeter-wave bands. *IEEE Commun. Mag.* **2014**, *52*, 78–86. [CrossRef]
11. Jilani, S.F.; Alomainy, A. Millimetre-wave T-shaped MIMO antenna with defected ground structures for 5G cellular networks. *IET Microwaves Antennas Propag.* **2018**, *12*, 672–677. [CrossRef]
12. Rahman, S.; Ren, X.c.; Altaf, A.; Irfan, M.; Abdullah, M.; Muhammad, F.; Anjum, M.R.; Mursal, S.N.F.; AlKahtani, F.S. Nature inspired MIMO antenna system for future mmWave technologies. *Micromachines* **2020**, *11*, 1083. [CrossRef] [PubMed]
13. Khalid, M.; Iffat Naqvi, S.; Hussain, N.; Rahman, M.; Mirjavadi, S.S.; Khan, M.J.; Amin, Y. 4-Port MIMO antenna with defected ground structure for 5G millimeter wave applications. *Electronics* **2020**, *9*, 71. [CrossRef]
14. Bilal, M.; Naqvi, S.I.; Hussain, N.; Amin, Y.; Kim, N. High-Isolation MIMO antenna for 5G millimeter-wave communication systems. *Electronics* **2022**, *11*, 962. [CrossRef]
15. Sehrai, D.A.; Abdullah, M.; Altaf, A.; Kiani, S.H.; Muhammad, F.; Tufail, M.; Irfan, M.; Glowacz, A.; Rahman, S. A novel high gain wideband MIMO antenna for 5G millimeter wave applications. *Electronics* **2020**, *9*, 1031. [CrossRef]
16. Tariq, S.; Naqvi, S.I.; Hussain, N.; Amin, Y. A metasurface-based MIMO antenna for 5G millimeter-wave applications. *IEEE Access* **2021**, *9*, 51805–51817. [CrossRef]

17. Sehrai, D.A.; Asif, M.; Shah, W.A.; Khan, J.; Ullah, I.; Ibrar, M.; Jan, S.; Alibakhshikenari, M.; Falcone, F.; Limiti, E. Metasurface-based wideband MIMO antenna for 5G millimeter-wave systems. *IEEE Access* **2021**, *9*, 125348–125357. [CrossRef]
18. Sehrai, D.A.; Asif, M.; Shoaib, N.; Ibrar, M.; Jan, S.; Alibakhshikenari, M.; Lalbakhsh, A.; Limiti, E. Compact quad-element high-isolation wideband MIMO antenna for mm-wave applications. *Electronics* **2021**, *10*, 1300. [CrossRef]
19. Patel, A.; Vala, A.; Desai, A.; Elfergani, I.; Mewada, H.; Mahant, K.; Zebiri, C.; Chauhan, D.; Rodriguez, J. Inverted-L Shaped Wideband MIMO Antenna for Millimeter-Wave 5G Applications. *Electronics* **2022**, *11*, 1387. [CrossRef]